Design of LD in-band direct-pumping side surface polished micro-rod Nd:YVO_4 laser

Wen-Qi Zhang(张文启), Fei Wang(王飞), Qiang Liu(柳强), and Ma-Li Gong(巩马理)†

State Key Laboratory of Tribology, Center for Photonics and Electronics, Department of Precision Instruments, Tsinghua University, Beijing 100084, *China*

(Received 8 April 2015; revised manuscript received 11 August 2015; published online 20 December 2015)

To diminish the thermal load, two ways, that is, in-band direct pumping and micro-rod crystal, could be adopted at the same time. The efficiency of LD in-band direct-pumping side surface polished micro-rod Nd:YVO_4 laser is numerically analyzed. By optimizing parameters such as crystal length, laser mode radius, pump beam radius, doping concentration and crystal cross-section size, the overall efficiency can reach over 50%. It is found that with micro-rod crystal implemented in the laser oscillator, high overall efficiency LD in-band direct-pumping Nd:YVO_4 laser could be realized. High efficiency combined with low thermal load makes this laser an outstanding scheme for building high-power Nd:YVO_4 lasers.

Keywords: diode-pumped lasers, design of specific laser systems, efficiency

PACS: 42.55.Xi, 42.60.By, 42.60.Lh **DOI:** 10.1088/1674-1056/25/2/024207

1. Introduction

The neodymium-doped vanadate (Nd:YVO_4) crystal is widely used as a laser medium in laser diode (LD) pumped solid-state laser due to its valuable properties such as polarized emission and high gain.[1,2] However, relatively poor thermal and mechanical characteristics strongly limit the pump power and the laser power, degrade the beam quality, or damage the crystal. Some ways were investigated to diminish the thermal load of the crystal. One way is to reduce the quantum defect with in-band direct pumping[3] to the upper lasing level such as at 880 nm[4] or 888 nm[5] instead of 808 nm. Splitting the thermal load with multiple crystals[6] is also a solution. Composite crystal[7,8] is another common method to relieve the thermal load. Changing the crystal shape into a disk,[9] or slab,[10] replacing the traditional rod is also an available option.

Single crystal fiber (SCF) is a long and thin crystal rod with a diameter usually smaller than 1 mm, a typical length of several centimeters and a cylindrical surface good enough to guide the pump beam by total internal reflection.[11] SCF is so designed that the laser beam propagates in the medium freely as does a traditional bulk laser, whereas the pump beam is guided by the thin crystal rod, which depends on the pump brightness.[12] Basically, single crystal fibers are grown by the laser heated pedestal growth technique.

Just like single crystal fiber, micro-rod crystal has a micro cross section with side surface polished good enough to guide the pump beam by total internal reflection and is a thin rod-shaped crystal whose cross section can be circular, elliptical, squared or other shapes. Micro-rod crystal possesses almost all the characteristics of single crystal fiber and has more cross section shapes to be chosen. The guiding characteristic of the pump beam enables longer gain medium with lower absorption coefficient to be used, resulting in reduced thermal load in the crystal. The large area-to-volume ratio of the micro-rod also diminishes crystal thermal load. The freely propagating property of the laser beam in the crystal facilitates the formation of a large mode area of the laser beam, which helps avoid non-linear effects. It is worth emphasizing that the micro-rod is processed mechanically as ordinary-sized crystal would be, which is different from SCF. The SCFs have been successfully implemented in Yb:YAG[13] and Nd:YAG[14] oscillators and pulsed Yb:YAG amplifiers. However, as we speculate, the Nd:YVO_4 single crystal fiber which is suitable for high efficiency laser may be difficulty to grow, so the Nd:YVO_4 single crystal fiber laser has not been reported so far.

To diminish the thermal load, two ways, that is, direct pumping and micro-rod crystal, could be adopted at the same time. Thin and long crystal can reduce thermal load but also reduce the overlap efficiency between laser mode and pump mode at the same time. What is the efficiency of LD in-band directly pumping micro-rod Nd:YVO_4 laser? In this paper, the efficiency of LD in-band direct-pumping side surface polished micro-rod Nd:YVO_4 laser is numerically analyzed. It is found that with micro-rod implemented in the laser oscillator, LD in-band direct-pumping high overall efficiency Nd:YVO_4 laser could be realized. Its high efficiency and low thermal load make it an outstanding scheme for high-power Nd:YVO_4 lasers.

2. Theoretical analysis and numerical simulations

Laser performance is typically characterized by slope efficiency. The slope efficiency σ_s of the output power versus

†Corresponding author. E-mail: gongml@mail.tsinghua.edu.cn

© 2016 Chinese Physical Society and IOP Publishing Ltd

input power curve is given as follows:[15]

$$\sigma_{\mathrm{S}} = \frac{2(1-R)}{(1+R)(L-\ln R)}\eta_{\mathrm{PS}}\eta_{\mathrm{T}}\eta_{\alpha}\eta_{\mathrm{Q}}\eta_{\mathrm{S}}\eta_{\mathrm{B}}, \tag{1}$$

where R is the reflectivity, L is the round-trip cavity-loss, η_{PS} is the pump source spectral efficiency, η_{T} is the transfer efficiency, η_{α} is the absorption efficiency, η_{Q} is the quantum efficiency, η_{S} is the quantum defect efficiency, and η_{B} is the beam overlap efficiency.

The pump source spectral efficiency η_{PS} is the fraction of input optical power which is in the absorption region of the gain medium.

The optical transfer efficiency η_{T} is the ratio between the optical power incident on the gain medium and that emitted by the pump source.

The absorption efficiency η_{α} is the ratio of the power absorbed in the gain medium to the power of entering the gain medium. For diode pumped laser, the absorption efficiency can be approximated, and given below.

$$\eta_{\alpha} = 1 - \exp(-\alpha l), \tag{2}$$

where α is the absorption coefficient, and l is the path length in the gain medium.

The quantum efficiency η_{Q} is defined as the number of photons contributing to laser emission, divided by the number of pump photons.

The quantum defect efficiency η_{S} is the Stokes factor which represents the ratio of the photon energy emitted at the laser to the energy of a pump photon, and expressed as.

$$\eta_{\mathrm{S}} = \frac{\lambda_{\mathrm{P}}}{\lambda_{\mathrm{L}}}, \tag{3}$$

where λ_{P} is the wavelength of the pump, and λ_{L} is the laser wavelength.

The beam overlap efficiency η_{B} is defined as the resonator mode volume divided by the pumped volume of the active gain medium,[16] and described as

$$\eta_{\mathrm{B}} = \frac{\left[\iiint s_{\mathrm{l}}(x,y,z)\, r_{\mathrm{p}}(x,y,z)\, \mathrm{d}V\right]^2}{\iiint s_{\mathrm{l}}^2(x,y,z)\, r_{\mathrm{p}}(x,y,z)\, \mathrm{d}V}, \tag{4}$$

where $s_{\mathrm{l}}(x,y,z)$ is the normalized cavity mode intensity distribution, and $r_{\mathrm{p}}(x,y,z)$ is the normalized pump intensity distribution in the active gain medium.

To obtain the beam overlap efficiency, a three-dimensional (3D) ray-tracing model is built to simulate optical intensity distribution in the active gain medium instead of a commonly used mathematical expression. For instance, it can be set that the micro-rod has a diameter of 1 mm, and is incident by a 888-nm Gaussian beam with a far field divergence angle of 0.11 and focal diameter of 400 μm in the front face of the crystal. The pump intensity distributions (normalized by the maximum of intensity) in the micro-rod crystal with side surface polished and traditional rod crystal with side surface unpolished are obtained respectively as shown in Fig. 1. The laser propagating in the crystal can be set to have a Gaussian profile with a mode diameter of 800 μm throughout this crystal. The calculated overlap efficiency as a function of axial position of the crystal is shown in Fig. 2. It can be seen that the overlap efficiency of the micro-rod crystal is different from one of traditional rod crystal, which decreases down first and reaches a minimum, which is corresponding to a position where a major part of the pump beam is reflected on the side surface, then increases to a certain level as the axial position increases.

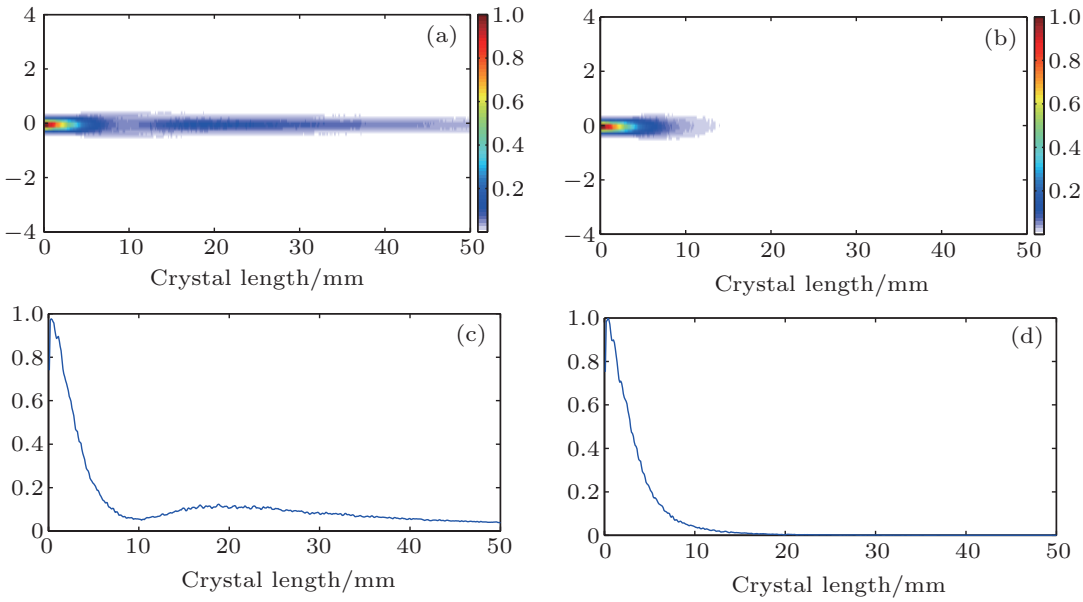


Fig. 1. (color online) Pump intensity distributions normalized by the maximum in a 1-mm-diameter 50-mm-long micro-rod crystal [(a) and (c)] and traditional rod crystal [(b) and (d)]. The 888-nm pump beam radius is 200-μm and the far field divergence angle is 0.11.

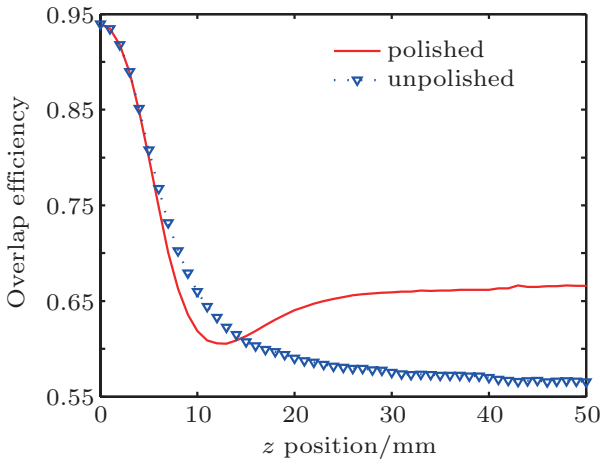


Fig. 2. (color online) Overlap efficiencies between the pump beam and an 800-μm diameter Gaussian-profile laser beam as a function of axial position for the micro-rod crystal with side surface polished and traditional rod crystal with side surface unpolished.

In order to compare the thermal effect of micro-rod crystal with that of traditional rod crystal, their temperature distributions are simulated. Large area-to-volume ratio makes the thermal effect of the micro-rod lower than that of traditional rod crystal, which is indicated in Fig. 3. In simulation, we assume that the pump power is 100 W, the micro-rod is 0.26 at.% doped cylinder with 1 mm in diameter and 50 mm in length, the traditional rods are 0.5 at.% and 0.26 at.% doped cylinders each with 3 mm in diameter and 30 mm in length.

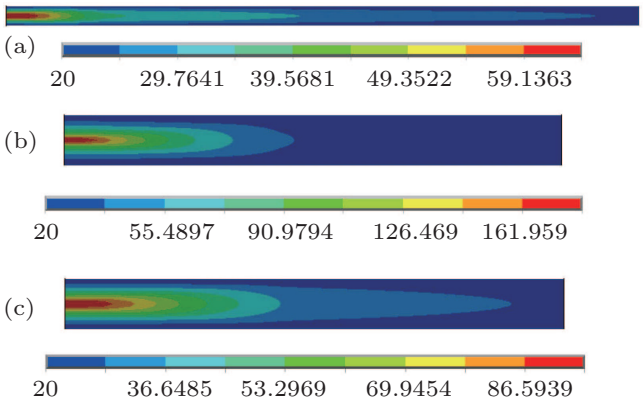


Fig. 3. (color online) Temperature distribution of the 0.26 at.% doped 1-mm-diameter and 50-mm-long micro-rod (a), 0.5 at.% doped 3-mm-diameter and 30-mm-long traditional rod crystal (b), and 0.26 at.% doped 3-mm-diameter and 30-mm-long traditional rod crystal (c).

3. Results and discussion

The schematic diagram of the simulated setup is shown in Fig. 4. The Nd:YVO_4 crystal is end-pumped by an LD, which has a pigtailed fiber with a diameter of 200 μm and a numerical aperture (NA) of 0.22. Unless otherwise specified, the following analyses by default use 888 nm as the pump wavelength and Nd:YVO_4 has a diameter of 1 mm and 0.26 at.% doped. The transmittance of the output coupler is optimized.

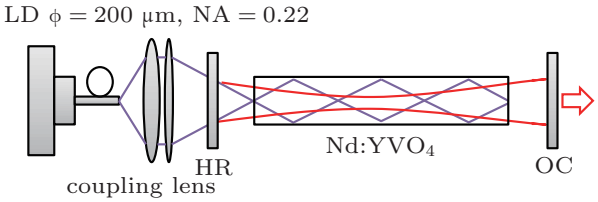


Fig. 4. (color online) Schematic diagram of simulated setup.

Figure 5 shows the relationship between overall efficiency and laser beam radius when the 888-nm pump beam radius is 200 μm. As can be seen from Fig. 5, with increasing laser beam radius, the efficiency increases till its maximum, and then drops down. This can be explained by the fact that the overlap efficiency is higher when the waist radius of the laser beam becomes greater, but the diffraction loss becomes larger at the same time.

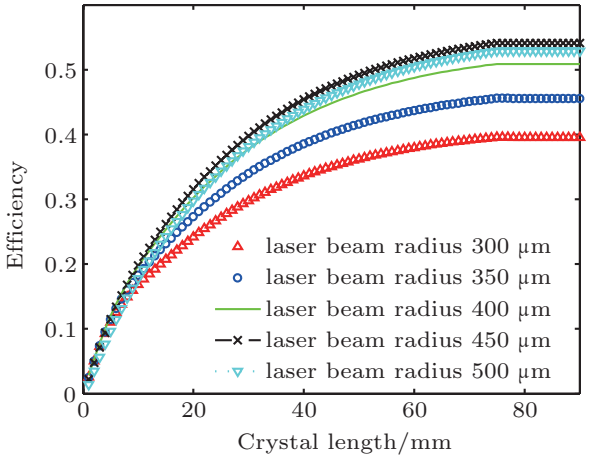


Fig. 5. (color online) Overall efficiencies as a function of crystal length for different laser beam radii when the pump beam radius is 200 μm.

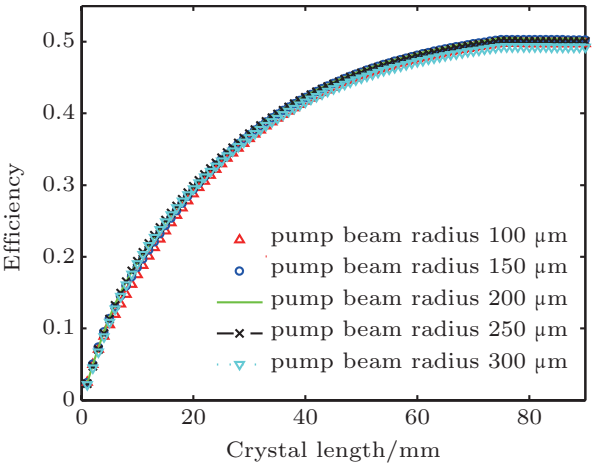


Fig. 6. (color online) Overall efficiencies as a function of crystal length for different pump beam radii when the laser beam radius is 400 μm.

Figure 6 shows the relationship between overall efficiency and pump radius defined at a focal spot when the laser beam radius is 400 μm. It can be seen that the pump radius has little effect on the overall efficiency. This is quite different from the scenario of the traditional LD-pumped Nd:YVO_4 laser, for

which the overlap efficiency reaches a certain value with the increase of distance in crystal.

Figure 7 shows the overall efficiencies as a function of crystal length with different doping concentrations when the laser beam radius is 400 μm and the pump beam radius is 200 μm. It can be seen that highly doped crystal is not a good choice. Although high doping concentration can lead to a good pump absorption of the same length, at the same time it will induce a significant cross relaxation, bring about strong Auger up-conversion and diminish the upper level lifetime, thereby reducing the overall efficiency.

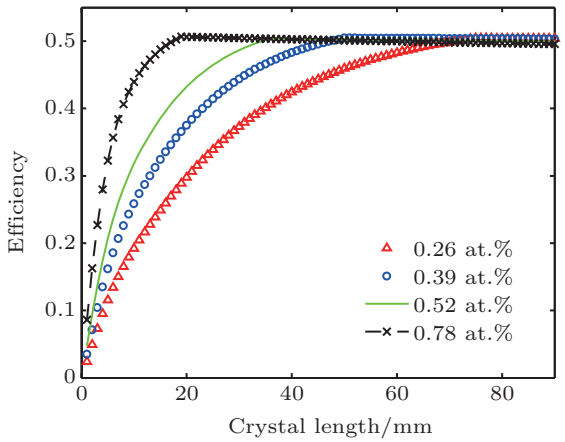


Fig. 7. (color online) Overall efficiencies as a function of crystal length with different doping concentrations when the laser beam radius is 400 μm and the pump beam radius is 200 μm.

Figure 8 shows the overall efficiencies as a function of crystal length with different crystal diameters. The pump beam radii are 100 μm, 200 μm, and 300 μm, and the laser beam radii are 200 μm, 400 μm, and 600 μm when crystal diameters are 0.5 mm, 1 mm, 1.5 mm. It can be seen that the size of the crystal cross section has little effect on the overall efficiency. For practical consideration, a preferable crystal diameter should be around 1 mm. For larger crystals, a correspondingly larger laser beam is required to achieve this efficiency, which is hard to realize in practice. For crystals with diameters that are too small, they can hardly be manufactured by current manufacturing techniques.

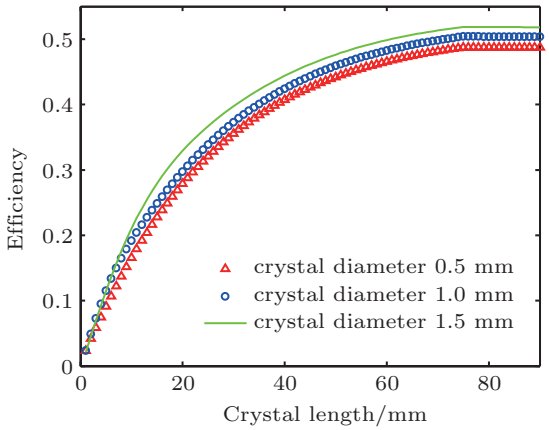


Fig. 8. (color online) Overall efficiencies as a function of crystal length with different crystal diameters. The pump beam radii are 100 μm, 200 μm, and 300 μm, and the laser beam radii are 200 μm, 400 μm, and 600 μm when crystal diameters are 0.5 mm, 1 mm, and 1.5 mm.

Comparisons of other published experimental results with numerical analyses are shown in Table 1. Yb:YAG single-crystal fiber continuous laser with 251-W output power and a slope efficiency of 53% is demonstrated.[13] To our knowledge, this is the highest power, highest slope efficiency ever reported on single-crystal fiber lasers. In the experiment, the pump diameter is 600 μm, the laser diameter is 700 μm, the Yb:YAG single-crystal fiber is 40-mm long and 1 mm in diameter with a low doping concentration of 1%. The absorption efficiency of 1% doped Yb:YAG for 940-nm pump is around 0.58 cm^{-1}, which is similar to that of the 0.39% doped Nd:YVO_4 for 888-nm pump. Comparing with the experimental results, we obtain a similar conclusion from the numerical analyses.

Table 1. Comparison between experimental results and numerical analyses.

Year	Gain medium	Pump	Laser	Output
2006[17]	Nd:YAG SCF long, 50-mm diameter, 1-mm doping, 0.2%	fiber-coupled, LD 60 W, 808 nm, 400 μm, NA 0.2	waist, 250 μm	CW, 1064 nm 10.2 W slope efficiency, 22%
2012[13]	Yb:YAG SCF long, 40-mm diameter, 1-mm doping, 1%	fiber-coupled, LD 600 W, 940 nm, 600 μm, NA 0.22	diameter, 700-μm	CW, 1030 nm 251 W slope efficiency, 53%
2013[12]	Yb:YAG SCF long, 40-mm diameter, 1-mm doping, 1%	fiber-coupled, LD 75 W, 940 nm, 105 μm, NA 0.15	seed beam diameter, 450 μm	CW, 1030 nm 20.5 W slope efficiency, 50%
Numerical analyses	Nd:YVO_4 micro-rod long, 60-mm diameter, 1-mm doping, 0.39%	fiber-coupled, LD 100 W, 888 nm, 200 μm, NA 0.22	diameter, 800-μm	CW, 1064-nm slope efficiency, over 50%

4. Conclusions

To diminish the thermal load, two ways, that is, in-band direct pumping and micro-rod crystal could be adopted at the same time. In-band direct pumping micro-rod Nd:YVO_4 lasers have not been reported so far to our knowledge. In this paper, the efficiencies of LD in-band direct-pumping side surface polished micro-rod Nd:YVO_4 lasers are numerically analyzed. By optimizing parameters such as crystal length,

laser mode radius, pump beam radius, doping concentration and crystal cross-section size, the overall efficiency can reach over 50%. It is found that with micro-rod crystal implemented in the laser oscillator, high overall efficiency LD in-band direct-pumping Nd:YVO_4 laser could be realized. High efficiency combined with low thermal load makes it an outstanding scheme for building high-power Nd:YVO_4 lasers. The following work is the experimental study of LD in-band direct-pumping micro-rod Nd:YVO_4 laser.

References

[1] Li X, Li G Q, Zhao S Z, Wang X M, Yin L, Huang H and Ma X M 2012 *Laser Phys.* **22** 673

[2] Du G L, Li G Q, Zhao S Z, Li T, Yang K J and Li X 2011 *Laser Phys.* **21** 1880

[3] Chang L, Yang C, Yi X J, Ai Q K, Chen L Y, Chen M, Li G, Yang J H and Ma Y F 2012 *Laser Phys.* **22** 1369

[4] Sato Y, Taira T, Pavel N and Lupei V 2003 *Appl. Phys. Lett.* **82** 844

[5] McDonagh L, Wallenstein R, Knappe R and Nebel A 2006 *Opt. Lett.* **31** 3297

[6] Chen Y F, Lan Y P and Wang S C 2000 *Opt. Lett.* **25** 1016

[7] Li T, Zhuo Z, Li X, Yang H and Zhang Y 2007 *Chin. Opt. Lett.* **5** 175

[8] Zhuo Z, Li T, Li X and Yang H 2007 *Chin. Opt. Lett.* **5** S13

[9] Millar P, Kemp A J and Burns D 2009 *Opt. Lett.* **34** 782

[10] Zhu P, Li D, Hu P, Schell A, Shi P, Haas C R, Wu N and Du K 2008 *Opt. Lett.* **33** 1930

[11] Piehler S, Délen X, Rumpel M, Didierjean J, Aubry N, Graf T, Balembois F, Georges P and Ahmed M A 2013 *Opt. Express* **21** 11376

[12] Délen X, Zaouter Y, Martial I, Aubry N, Didierjean J, Hönninger C, Mottay E, Balembois F and Georges P 2013 *Opt. Lett.* **38** 109

[13] Délen X, Piehler S, Didierjean J, Aubry N, Voss A, Ahmed M A, Graf T, Balembois F and Georges P 2012 *Opt. Lett.* **37** 2898

[14] Délen X, Martial I, Didierjean J, Aubry N, Sangla D, Balembois F and Georges P 2011 *Appl. Phys. B: Lasers and Optics* **104** 1

[15] Koechner W 2006 *Solid-state laser engineering*, 6nd edn. (New York: Springer) p. 105

[16] Laporta P and Brussard M 1991 *IEEE J. Quantum Electron.* **27** 2319

[17] Didierjean J, Castaing M, Balembois F, Georges P, Perrodin D, Fourmigué J M, Lebbou K, Brenier A and Tillement O 2006 *Opt. Lett.* **31** 3468